

# Multi-faceted Graph Attention Network for Radar Target Recognition in Heterogeneous Radar Network

Han Meng<sup>a</sup>, Yuxing Peng<sup>a,\*\*</sup>, Wei Xiang<sup>b</sup>, Xu Pang<sup>a</sup>, and Wenbo Wang<sup>a,\*\*</sup>

<sup>a</sup>Beijing University of Posts and Telecommunications, Beijing, China

<sup>b</sup>La Trobe University, Melbourne, VIC, Australia

**Keywords:**

Radar target recognition

graph attention network  
attention mechanism  
semantic feature fusion

## ABSTRACT

Radar target recognition (RTR), as a key technology of intelligent radar systems, has been well investigated. Accurate RTR at low signal-to-noise ratios (SNRs) still remains an open challenge. Most existing methods are based on a single radar or the homogeneous radar network, which do not fully exploit frequency-dimensional information. In this paper, a two-stream semantic feature fusion model, termed Multi-faceted Graph Attention Network (MF-GAT), is proposed to greatly improve the accuracy in the low SNR region of the heterogeneous radar network. By fusing the features extracted from the source domain and transform domain via a graph attention network model, the MF-GAT model distills higher-level semantic features before classification in a unified framework. Extensive experiments are presented to demonstrate that the proposed model can greatly improve the RTR performance at low SNRs.

## 1. Introduction

Radar target recognition (RTR) is a critical component of modern radar technology, with applications in aviation and other wide-ranging fields. The major concerns of RTR mainly relate to data acquisition, semantic feature discovery and extraction technology. High-resolution signals like high-resolution range profile (HRRP) [1, 2], synthetic aperture radar (SAR) images [3], and inverse synthetic aperture radar (ISAR) images [4] present rich information of targets but demand powerful radar. The radar cross section (RCS) signal, which characterizes the scattering shape and the movement pattern of the target, is widely used due to its easy availability and sufficient information for RTR. As a result, the RCS signal is employed for RTR in this study.

RCS signals vary with frequency, illumination directions of the incident wave, scattering coefficient of the surface material, etc [5]. It is crucial to reliably extract semantic features from the

RCS signal for the purpose of RTR. RCS-based RTR methods can be roughly categorized into the traditional and deep learning based methods. Traditional methods try to detect some special feature parameters to recognize targets. In [6], 14 statistical features are extracted and a greedy algorithm is employed to discover the best combination of the extracted features for RTR. Besides statistical methods, transform domain methods are also widely applied. In [7] 10 statistical features are extracted from the RCS and transform domain via the Mellin transform and then the support vector machine (SVM) and Multi-layer perceptron (MLP) are employed for target recognition. Wang et al. [5] extract 5 statistical features via the wavelet transform and establish a set-valued model to represent the correlation between the feature vector and the authenticity of the radar target. There are many methods extracting angular diversity features [8, 9] with physical significance. When features are extracted, several classification criteria are established. In [10], the central moments of the RCS are extracted from different radar targets and then classified via the principal component analysis (PCA) and SVM. In [11], the K-nearest neighbors (KNN) regression method is employed for RTR.

Traditional methods usually demand features engineering and cannot fully extract abstract semantic features. By contrast, deep learning-based methods exhibit superior end-to-end

<sup>\*\*</sup>Corresponding Author

*e-mail:* menghan@bupt.edu.cn (Han Meng),  
yxpeng@bupt.edu.cn (Yuxing Peng),  
w.xiang@latrobe.edu.au (Wei Xiang), pengxu\_6@bupt.edu.cn  
(Xu Pang), wbwang@bupt.edu.cn (and Wenbo Wang)

learning and abstract representation capabilities. There exist many popular deep learning models, such as the recurrent neural network (RNN) [2, 12, 13], generative adversarial network (GAN) [14], and convolutional neural network (CNN) [3]. In [15], a CNN-based RCSNet model is proposed to classify different targets with the same shape. Wengrowski et al. [16] simulate the RCS signals of rotating and tumbling targets with unknown motion parameters, and then classify them using a CNN model. The aforementioned methods mainly have two shortcomings, i.e., the dependence on a well-annotated dataset with large volume and variety, and inability to fully exploit inherent semantic features and thus a relatively poor recognition performance at low signal-to-noise ratios (SNRs) when they are based on a single radar or a homogeneous radar array.

A radar array can provide spatial information for RTR. Graph convolutional network (GCN)-based models [17] are investigated recently. It is well known that GCN models depend heavily on the design of the adjacent matrix, which defines the correlation between any two nodes. Existing adjacent matrix design methods are based upon geographical distances [18] or the operating frequencies of the radars [19]. In the task of RTR, the correlation of the RCS signals at two nodes may does not depend on the geographical distance or operating frequency. In the semantic space, it depends on the observed target. That is, the RCS signals should be highly correlated when the two radars observe the same target regardless of the operating mode or spatial location. In this sense, the semantic similarity in the semantic space should be defined and learned in the GCN model, which facilitates the extension of RTR in the heterogeneous network to extract more information when compared with homogeneous network-based methods.

In this study, a new RTR model, termed the Multi-faced Graph Attention Network (MF-GAT), is developed for heterogeneous radar arrays, where spatially distributed radars may work in different operating modes in terms of operating frequency, bandwidth, pulse width, and pulse repetition interval. The proposed model facilitates the semantic feature extraction in a transform domain by a specifically designed parallel branch, and then fuse features from two branches in the semantic space before deeper abstract feature extraction. Through feature enhancement, the proposed model can greatly improve the RTR performance in the low SNR range.

The rest of the paper is organized as follows. Section 2 presents the signal and system models. Section 3 describes the proposed MFGAT model in detail. Section 4 presents experimental results and analysis, followed by concluding remarks drawn in Section 5.

## 2. System Model

A heterogeneous radar network includes  $N$  spatially distributed radars with different operating modes and  $M$  flight targets. These radars detect targets independently and constitute a heterogeneous radar array. From the echoes in the form of the RCS, target information such as the scattering shape and movement pattern can be inferred using advanced signal processing.

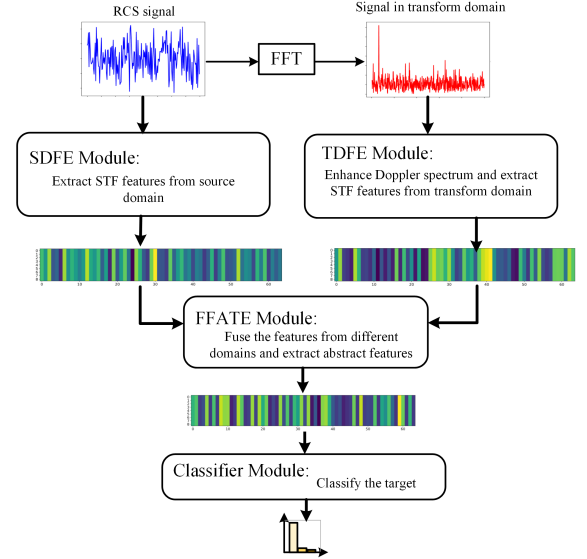


Fig. 1: The flow chart of the MF-GAT.

According to electromagnetic theory, the RCS is given by

$$g = \lim_{R \rightarrow \infty} 4\pi R^2 \left| \frac{E_s}{E_i} \right|^2, \quad (1)$$

where  $R$  is the distance from the radar to target,  $E_s$  and  $E_i$  are the scatter field intensity and the incident field intensity, respectively. The RCS is highly influenced by such factors as the carrier frequency and polarization mode of the incident electromagnetic wave, incident angle, surface shape, and scattering coefficient of the target.

During the observation period, the detection range varies with the movement of the target, resulting in fast variations of the received SNR. The received signal can be expressed as

$$x(t) = \alpha(t)g(t) + n(t), \quad (2)$$

where  $\alpha(t)$  is the attenuation factor,  $g(t)$  is the time varying RCS given by Equation 1, and  $n(t)$  is the additional white Gaussian noise with zero mean and a variance of  $\sigma_n^2$ . Then the SNR at the transmitter (TSNR) is defined as  $TSNR = \frac{E\{|g|^2\}}{E\{|n|^2\}}$ , and the SNR at the receiver (RSNR) is defined by  $RSNR = E\{|\alpha(t)|^2\} \cdot TSNR$ .

The heterogeneous radar network is modeled as a undirected graph  $G = (X, A)$ , where the node feature set  $X$  represents the RCS signals at the  $N$  radars, and the correlation among the radars is represented by the adjacency matrix  $A$ , which demands to learn the semantic similarity between RCS signals of  $N$  radars. Based on the heterogenous radar array, the RTR model tries to learn the mapping from the RCS signals to the classification of the observed targets. That is, given RCS signals  $X$ , the RTR task can be formulated as  $Y = F(X)$ , where  $Y$  denotes the target class label and  $F$  denotes the mapping function.

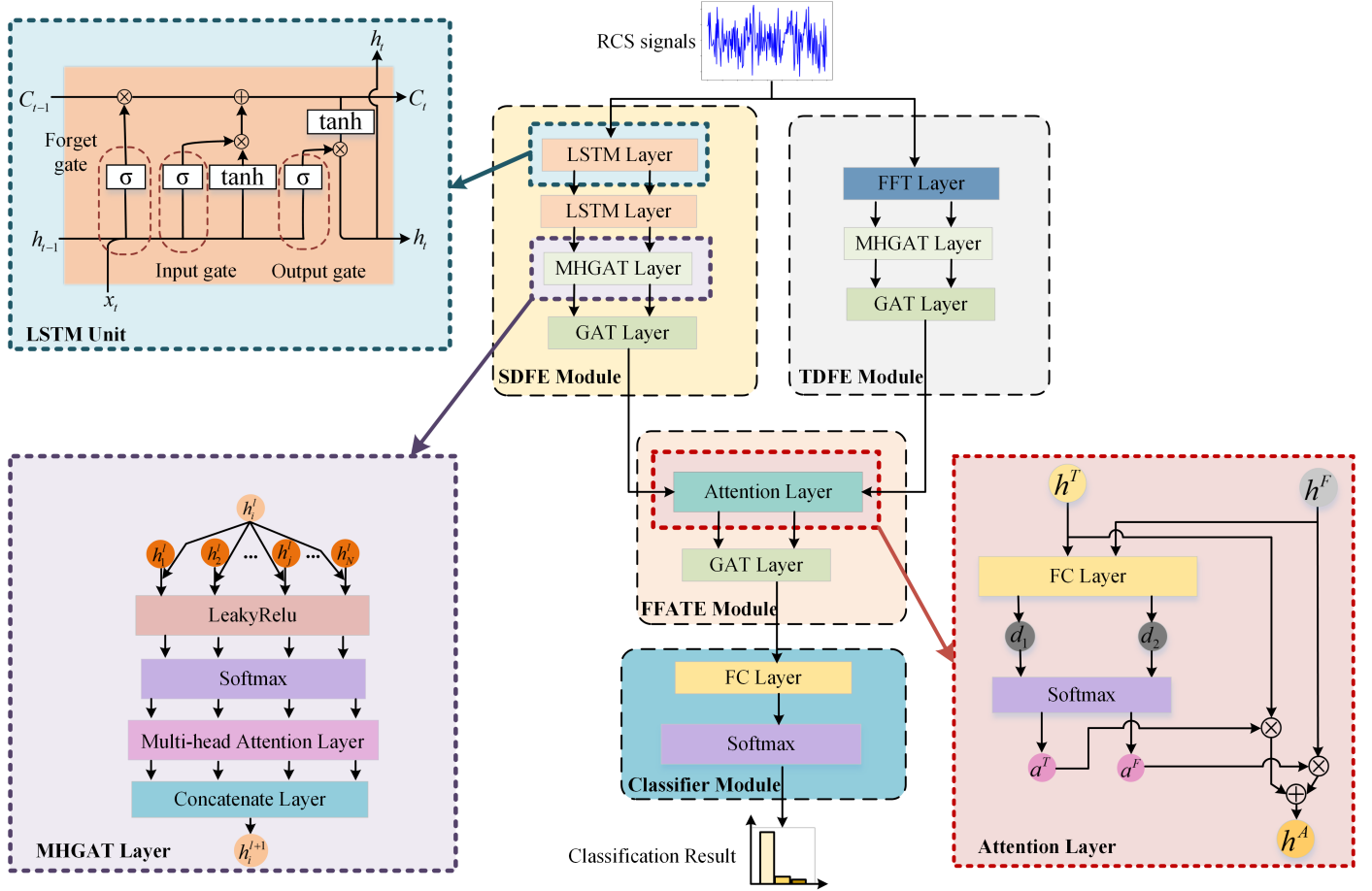


Fig. 2: The network structure of the MF-GAT.

### 3. MF-GAT Model

In this section, the proposed MF-GAT model is introduced. As depicted in Fig. 1, the MF-GAT model consists of four modules, including two feature extraction modules, a feature fusion and abstract feature extraction (FFATE) module, and a classifier module. The first feature extraction module extracts semantic features directly from the RCS, which is termed the source domain feature extraction (SDFE) module, while the parallel transform domain feature extraction module termed TDFE extracts semantic features from the transform domain using the fast Fourier transform (FFT). Since the Doppler spectrum is one of the most important feature for moving target recognition, it is necessary to facilitate feature extraction module by presenting signals in frequency domain.

The detailed network structure is shown in Fig. 2, in which each module is detailed subsequently.

#### 3.1. SDFE Module

The SDFE module extracts temporal domain features by the long short-term memory (LSTM) network, and then dynamically models the spatial dependencies among the radars by a graph attention network with multi-head attention mechanism (MHGAT) [20], finally fuses multi-domain features using a graph attention network (GAT).

#### 3.1.1. Temporal Dependency Modeling

The LSTM network is employed to extract temporal features. An LSTM network is composed of one or more LSTM layers, and each LSTM layer consists of several LSTM units, which includes three gates, i.e., the forget gate  $U$ , input gate  $I$ , and output gate  $O$ . The operations in an LSTM unit are described below.

$$O_{t,i} = \sigma(W_{O,i}[h_{t-1,i}; x_{t,i}] + b_{O,i}), \quad (3)$$

$$I_{t,i} = \sigma(W_{I,i}[h_{t-1,i}; x_{t,i}] + b_{I,i}), \quad (4)$$

$$U_{t,i} = \sigma(W_{U,i}[h_{t-1,i}; x_{t,i}] + b_{U,i}), \quad (5)$$

$$\tilde{C}_{t,i} = \tanh(W_{C,i}[h_{t-1,i}; x_{t,i}] + b_{C,i}), \quad (6)$$

$$C_{t,i} = U_{t,i} \otimes C_{t-1,i} + I_{t,i} \otimes \tilde{C}_{t,i}, \quad (7)$$

$$h_{t,i} = O_{t,i} \otimes \tanh(C_{t,i}), \quad (8)$$

where  $h_{t-1}$  and  $h_t$  are the input and output of the LSTM unit, respectively;  $W_U$ ,  $W_I$ , and  $W_O$  are the weight matrices to be learnt;  $b_U$ ,  $b_I$ , and  $b_O$  are the corresponding bias vectors to be learnt;  $\tilde{C}_{t,i}$  and  $C$  represent a candidate for cell state and the cell state, respectively.

### 3.1.2. Spatial Dependency Modeling

Some existing GCN models [18, 21] consider fixed spatial dependencies according to the geographic distances among nodes in a topology graph. In our model, the semantic similarity of nodes is learned by the GAT, which differs from the GCN in the feature aggregation manner among the neighboring nodes. For a GCN method, the feature aggregation operation returns the standardized sum of the neighbors' features as follows

$$h_i^{l+1} = \sigma\left(\sum_{j \in D_i} \frac{1}{c_{ij}} W^l h_j^l\right), \quad (9)$$

where  $\sigma$  is the activation function;  $D_i$  is the set of radars which are neighbors of the  $i$ -th radar;  $c_{ij}$  is a normalized constant based on the graph structure;  $l$  is the layer index;  $W^l$  is a shared weight matrix for feature transformation; and  $h_i^l$  is the hidden feature of the  $l$ -th layer for node  $i$ .

Based on GCN, GAT learns and weights the semantic features via attention mechanism. The mapping from output  $h_i^l$  of the  $l$ -th layer to the next layer output  $h_i^{l+1}$  is shown to be

$$z_i^l = W^l h_i^l, \quad (10)$$

$$e_{ij}^l = \text{LeakyReLU}(a^l(z_i^l \parallel z_j^l)), \quad (11)$$

$$a_{ij}^l = \frac{\exp(e_{ij}^l)}{\sum_{p \in D_i} \exp(e_{ip}^l)}, \quad (12)$$

$$h_i^{l+1} = \sigma\left(\sum_{j \in D_i} a_{ij}^l z_j^l\right). \quad (13)$$

Equation 10 uses a learnable weight matrix  $W^l$  to represent a linear combination of output  $h_i^l$ . In Equation 11, a pair-wise unnormalized attention score  $e_{ij}^l$  between radars  $i$  and  $j$  is computed through additive attention, which is performed by concatenating  $z_i^l$  and  $z_j^l$  via dot product and then weighting the output via a learnable weight vector  $a^l$  and the Leaky Rectified Linear Unit (LeakyReLU) activation function [22]. The output is normalized by a softmax activation function in Equation 12. In Equation 13, similar to the GCN, the higher layer output  $h_i^{l+1}$  is aggregated by the attention scores from neighbors.

To improve the model and stabilize the self-attention learning process, a multi-head attention mechanism [23] is employed, which allows the model to simultaneously learn the attention scores from various representation sub-spaces. The MHGAT contains independent  $K$  multi-head attention mechanisms that execute the GAT convolution operation simultaneously as shown in Fig. 2. The features are then concatenated to yield the feature representation as follows

$$h_i^{l+1} = \parallel_{k=1}^K \sigma\left(\sum_{j \in D_i} \alpha_{ij}^k W^k h_j^l\right), \quad (14)$$

where  $\parallel$  represents the concatenation operation.

Both the GAT and MHGAT layers are constructed to extract the spatial correlation among nodes and coherent temporal patterns hidden in the temporal domain.

### 3.2. TDFE Module

In order to explore features in the Doppler spectrum, the FFT is performed on the RCS signal to facilitate Doppler spectrum feature extraction by the TDFE module, which is formulated as

$$F(m) = \sum_{n=0}^{N-1} g_{real}(n) W_N^{mn}, m = 0, 1, \dots, N-1, \quad (15)$$

where  $W_N = \exp(-j2\pi/N)$ .

As shown in Fig. 2, the TDFE module contains the same MHGAT and GAT layers as SDFE. These layers extract the temporal-spatial-frequency features in the transform domain.

### 3.3. FFATE Module and Classifier Module

As illustrated in Fig. 2, extracted features from the SDFE and TDFE modules are fused by attention mechanism, and then higher semantic features are distilled through the GAT layer in the FFATE module. The features are fused as follows

$$h^A = a^T h^T + a^F h^F, \quad (16)$$

where  $a^T$  and  $a^F$  are the attention weights defined by

$$a^S = \text{softmax}(\tanh(W^T h^T + b^T)), \quad (17)$$

$$a^F = \text{softmax}(\tanh(W^F h^F + b^F)). \quad (18)$$

After feature fusion, the semantic features are continually updated by the GAT layer.

In the classifier module, the high-level semantic features are combined through a fully-connected layer, and finally the class label is yielded by the softmax layer.

## 4. Experimental Results and Discussions

### 4.1. Dataset and Data Preprocessing

The dataset under consideration contains RCS signals received by 9 radar of two types. All the radars independently detect two flight targets. The experimental settings are listed in Table 1. It is assumed that a radar can detect not more than one flight at a time. Then there are three scenarios for each radar, i.e., (1) no target; (2) target A; and (3) target B. The RSNR at each radar varies dynamically due to target movements.

Table 1: Experimental parameters.

Parameters	Values
Number of type-1 radar	5
Number of type-2 radar	4
Bandwidth of radar (MHz)	10
Pulse interval of radar (ms)	50
Operating frequency of type-1 radar (GHz)	3.25
Operating frequency of type-1 radar (GHz)	2.52
Mass trajectory (km/s)	5
Micro-motion frequency of type-1 aircraft (Hz)	0.64, 2.75
Micro-motion frequency of type-2 aircraft (Hz)	1.67, 8.72

In the dataset, each RCS signal segment includes 105000 samples. The samples are generated by a sliding window method. The size of sliding window is 200 of 10 seconds and the stride is 50. Then 6300 samples are obtained, which are randomly divided into the training, validation and test sets with a ratio of 7:2:1. Finally, all samples are normalized by a zero-mean normalization method.

#### 4.2. Baseline Models and Experimental Settings

Table 2: Experiment hyper-parameters.

Hyper-parameters	Values
Input units of LSTM	200
Hidden units of LSTM	128
Number of training epochs	100
Initial Learning rate	0.0005
Dropout probability	0.6
Optimizer	Adam
Batch size	32
Loss function	CrossEntropyLoss
Attention heads in MHGAT	8

All the comparative models are evaluated by Pytorch on NVIDIA GeForce GTX 3090. The experimental hyper-parameter settings are listed in Table 2. The employed performance evaluation metric is accuracy, which is define by

$$Accuracy = \frac{TP + TN}{TP + TN + FP + FN}, \quad (19)$$

where  $TP$  and  $TN$  are the correct numbers of positive samples and negative samples, respectively.  $FP$  and  $FN$  are the incorrect numbers of positive samples and negative samples, respectively. .

The compared baseline models include the following:

- Temporal dimension model: LSTM [24]
- Frequency dimension model: FFT-based CLEAN [25]
- Temporal-spatial (TS) dimension model: STGCN [18],
- Temporal-spatial-frequency (TSF) dimension algorithm: STFGACN [19].

#### 4.3. Main Results

The experimental results on accuracy versus the TSNR in dB are shown in Fig. 3. As stated before, the RSNR varies independently among radars due to the distance changes continuously caused by target movements. As a result, the TSNR is considered instead for fair comparison. In our experiments, the RSNR values are 7.5 dB below than the TSNR on average.

It can be observed from Fig.3:

- The proposed MF-GAT model outperforms all the reference models in the entire RSNR region, especially at low SNRs. . Specifically, at the low TSNR of 0 dB, the MT-GAT achieves 71.0% accuracy, which is 20.0%, 18.5%, 8.8%, 7.5% better than the FFT-based CLEAN, LSTM, STGCN, STFGACN models, respectively.

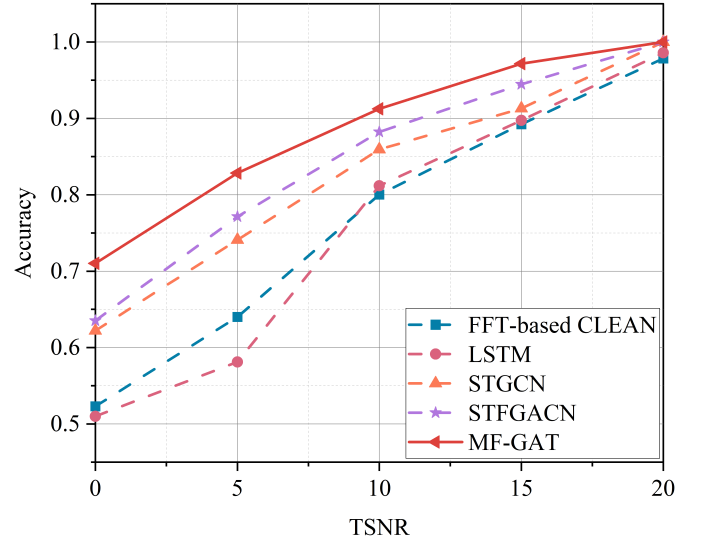


Fig. 3: Accuracy performance comparison.

- GCN-based multi-dimension models, including STGCN, STFGACN and MF-GAT, achieve better and more stable performance than single dimension models like FFT-based CLEAN and LSTM. This validates the fact that extracting features from multiple dimensions is able to improve accuracy, and the improvement increases with the dimension of domains. This is further verified by the results that STFGACN and MF-GAT behave better than STGCN.
- The gain in accuracy achieved by the proposed model increases with the decrease of SNR. Compared to the STFGACN model that extracts semantic features in the same temporal-spatial-frequency domain, the proposed MT-GAT model benefits from the extra parallel branch to extract the most critical Doppler spectrum feature in the transform domain, which results in the an evident improvement in RTR at low SNRs.
- By achieving the accuracy of 0.85, the MT-GAT achieves 3 dB and over 5 dB SNR gains over the GCN-based models and other models, respectively. The SNR gains can be translated into a longer detection range, which is vital for RTR.

#### 4.4. Ablation Studies

Ablation experiments are carried out to shed more light on the performance gains incurred by the functional modules in the MF-GAT model, i.e., the parallel branch and the multi-faceted fusing module. Three variants of the MF-GAT model are evaluated as follows:

- Baseline model, denoted by SDFE, only contains the SDFE and classifier modules, which extracts semantic features from the RCS signal directly.
- Baseline + TDFE, denoted by STDFFE, contains both the TDFE and SDFE modules, but the FFATE module is replaced by the concatenation operation, which means features from the TDFE and SDFE modules are concatenated via channel fusion.

- Baseline + TDFE + FFATE, denoted by MF-GAT, is the complete model.

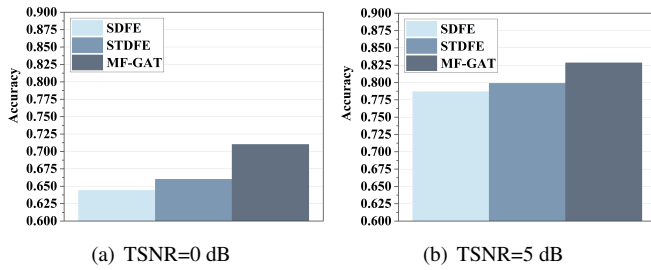


Fig. 4: Ablation studies on different components.

Fig. 4 presents the ablation results on the accuracy of RTR in two TSNR settings. As can be observed from the figure, the TDFE and FFATE modules can provide 1.2% and 2.9% accuracy enhancement at the TSNR of 5 dB, respectively, and the performance gains increase to 1.6% and 5% at the TSNR of 0 dB. Obviously, at the low SNRs, the extra parallel branch and the semantic feature fusion by the FFATE module are able to make RTR more reliable and more accurate.

## 5. Conclusion

In this paper, the MF-GAT model was proposed with the objective of greatly improving the accuracy of the RTR task in low SNR on a heterogeneous radar arrays at low SNRs. The proposed MF-GAT benefits from both the information dimension extension to temporal-spatial-frequency dimension and the extraction of Doppler spectrum features in the transform domain. Both comparative experimental and ablation results were presented to verify that the proposed MF-GAT model can reliably extract semantic features at low SNRs such that more accurate RTR is achieved.

## Acknowledgments

This work is supported by NSFC under grant 62071063.

## References

- [1] B. Feng, B. Chen, H. Liu, Radar HRRP target recognition with deep networks, *Pattern Recognition* 61 (2017) 379–393.
- [2] B. Xu, B. Chen, J. Wan, H. Liu, L. Jin, Target-aware recurrent attentional network for radar HRRP target recognition, *Signal Processing* 155 (2019) 268–280.
- [3] R. Xue, X. Bai, F. Zhou, Spatial-temporal ensemble convolution for sequence SAR target classification, *IEEE Transactions on Geoscience and Remote Sensing* 59 (2020) 1250–1262.
- [4] Y. Luo, Q. Zhang, C.-w. Qiu, X.-j. Liang, K.-m. Li, Micro-doppler effect analysis and feature extraction in ISAR imaging with stepped-frequency chirp signals, *IEEE Transactions on Geoscience and Remote Sensing* 48 (2009) 2087–2098.
- [5] T. Wang, W. Bi, Y. Zhao, W. Xue, Radar target recognition algorithm based on RCS observation sequence—set-valued identification method, *Journal of Systems Science and Complexity* 29 (2016) 573–588.
- [6] X. Lei, X. Fu, C. Wang, M. Gao, Statistical feature selection of narrow-band RCS sequence based on greedy algorithm, in: *Proceedings of 2011 IEEE CIE International Conference on Radar*, volume 2, IEEE, 2011, pp. 1664–1667.
- [7] W. Tang, L. Yu, Y. Wei, P. Tong, Radar target recognition of ballistic missile in complex scene, in: *2019 IEEE International Conference on Signal, Information and Data Processing (ICSIDP)*, IEEE, 2019, pp. 1–6.
- [8] S.-C. Chan, K.-C. Lee, Radar target recognition by MSD algorithms on angular-diversity RCS, *IEEE Antennas and Wireless Propagation Letters* 12 (2013) 937–940.
- [9] S.-C. Chan, K.-C. Lee, Angular-diversity target recognition by kernel scatter-difference based discriminant analysis on RCS, *International Journal of Applied Electromagnetics and Mechanics* 42 (2013) 409–420.
- [10] E. Gökkaya, T. Günel, A novel hybrid approach for radar target classification based on SVM and central moments with PCA using rcs, in: *2019 11th International Conference on Electrical and Electronics Engineering (ELECO)*, IEEE, 2019, pp. 575–579.
- [11] K.-C. Lee, Radar target recognition by machine learning of k-nearest neighbors regression on angular diversity RCS, *The Applied Computational Electromagnetics Society Journal (ACES)* (2019) 75–81.
- [12] L. Ye, S. Hu, T. Yan, X. Meng, M. Zhu, R. Xu, Radar target shape recognition using a gated recurrent unit based on RCS time series' statistical features by sliding window segmentation, *IET Radar, Sonar & Navigation* 15 (2021) 1715–1726.
- [13] J. Geng, H. Wang, J. Fan, X. Ma, SAR image classification via deep recurrent encoding neural networks, *IEEE Transactions on Geoscience and Remote Sensing* 56 (2017) 2255–2269.
- [14] C. He, D. Xiong, Q. Zhang, M. Liao, Parallel connected generative adversarial network with quadratic operation for SAR image generation and application for classification, *Sensors* 19 (2019) 871.
- [15] J. Chen, S. Xu, Z. Chen, Convolutional neural network for classifying space target of the same shape by using RCS time series, *IET Radar, Sonar & Navigation* 12 (2018) 1268–1275.
- [16] E. Wengrowski, M. Purri, K. Dana, A. Huston, Deep CNNs as a method to classify rotating objects based on monostatic RCS, *IET Radar, Sonar & Navigation* 13 (2019) 1092–1100.
- [17] T. N. Kipf, M. Welling, Semi-supervised classification with graph convolutional networks, in: *Proceedings of International Conference on Learning Representations*, 2017.
- [18] B. Yu, H. Yin, Z. Zhu, Spatio-temporal graph convolutional networks: A deep learning framework for traffic forecasting, in: *Proceedings of International Joint Conference on Artificial Intelligence*, 2018, pp. 3634–3640.
- [19] H. Meng, Y. Peng, W. Wang, P. Cheng, Y. Li, W. Xiang, Spatio-temporal-frequency graph attention convolutional network for aircraft recognition based on heterogeneous radar network, *IEEE Transactions on Aerospace and Electronic Systems* (2022).
- [20] P. Veličković, G. Cucurull, A. Casanova, A. Romero, P. Liò, Y. Bengio, Graph attention networks, in: *Proceedings of International Conference on Learning Representations*, 2018.
- [21] Z. Wu, S. Pan, G. Long, J. Jiang, C. Zhang, Graph wavenet for deep spatial-temporal graph modeling, in: *Proceedings of the 28th International Joint Conference on Artificial Intelligence*, 2019, pp. 1907–1913.
- [22] B. Xu, N. Wang, T. Chen, M. Li, Empirical evaluation of rectified activations in convolutional network, in: *Proceedings of the 32th International Conference on Machine Learning: Deep Learning Workshop*, 2015.
- [23] A. Vaswani, N. Shazeer, N. Parmar, J. Uszkoreit, L. Jones, A. N. Gomez, Ł. Kaiser, I. Polosukhin, Attention is all you need, *Advances in neural information processing systems* 30 (2017).
- [24] B. Sehgal, H. S. Shekhawat, S. K. Jana, Automatic target recognition using recurrent neural networks, in: *2019 International Conference on Range Technology (ICORT)*, IEEE, 2019, pp. 1–5.
- [25] I.-S. Choi, S.-J. Lee, Bistatic radar target identification using FFT-based CLEAN, in: *2014 IEEE Geoscience and Remote Sensing Symposium*, IEEE, 2014, pp. 1825–1828.